

Tuning a distributed feedback laser with a coupled microcavity

Lukas Mahler,¹ Alessandro Tredicucci,^{1,*} Fabio Beltram,¹ Harvey E. Beere,²
and David A. Ritchie²

¹NEST, Istituto Nanoscienze - CNR and Scuola Normale Superiore, Piazza San Silvestro 12, I-56127, Pisa, Italy

²Cavendish Laboratory, University of Cambridge, J J Thomson Avenue, Cambridge CB3 0HE, UK

*a.tredicucci@sns.it

Abstract: We show that a distributed-feedback terahertz quantum cascade laser can be tuned with a coupled microcavity by anti-crossing of the respective eigenfrequencies. In this proof-of-concept experiment, a tuning range of 20 GHz is obtained, in good agreement with a simple finite element model, which shows that the tuning is determined by the coupling strength between the resonators. The concept could be applied to any laser cavity, but becomes progressively more attractive the lower the emission frequency.

©2010 Optical Society of America

OCIS codes: (140.3070) Infrared and far-infrared lasers; (140.3490) Lasers, distributed-feedback; (140.5965) Semiconductor lasers, quantum cascade; (140.3410) Laser resonators; (140.3945) Microcavities; (140.3600) Lasers, tunable.

References and links

1. R. Köhler, A. Tredicucci, F. Beltram, H. E. Beere, E. H. Linfield, A. G. Davies, D. A. Ritchie, R. C. Iotti, and F. Rossi, "Terahertz semiconductor-heterostructure laser," *Nature* **417**(6885), 156–159 (2002).
2. B. S. Williams, "Terahertz quantum-cascade lasers," *Nat. Photonics* **1**(9), 517–525 (2007).
3. J. Xu, J. M. Hensley, D. B. Fenner, R. P. Green, L. Mahler, A. Tredicucci, M. G. Allen, F. Beltram, H. E. Beere, and D. A. Ritchie, "Tunable terahertz quantum cascade lasers with an external cavity," *Appl. Phys. Lett.* **91**(12), 121104 (2007).
4. A. W. M. Lee, B. S. Williams, S. Kumar, Q. Hu, and J. L. Reno, "Tunable terahertz quantum cascade lasers with external gratings," *Opt. Lett.* **35**(7), 910–912 (2010).
5. L. A. Dunbar, R. Houdré, G. Scalari, L. Sirigu, M. Giovannini, and J. Faist, "Small optical volume terahertz emitting microdisk quantum cascade lasers," *Appl. Phys. Lett.* **90**(14), 141114 (2007).
6. J. M. Hensley, J. Montoya, M. G. Allen, J. Xu, L. Mahler, A. Tredicucci, H. E. Beere, and D. A. Ritchie, "Spectral behavior of a terahertz quantum-cascade laser," *Opt. Express* **17**(22), 20476–20483 (2009).
7. Q. Qin, B. S. Williams, S. Kumar, J. L. Reno, and Q. Hu, "Tuning a terahertz wire laser," *Nat. Photonics* **3**(12), 732–737 (2009).
8. G. Scalari, C. Walther, M. Fischer, R. Terazzi, H. Beere, D. Ritchie, and J. Faist, "THz and sub-THz quantum cascade lasers," *Laser Photon. Rev.* **3**(1–2), 45–66 (2009).
9. L. Mahler, A. Tredicucci, F. Beltram, C. Walther, J. Faist, H. E. Beere, and D. A. Ritchie, "High-power surface emission from terahertz distributed feedback lasers with a dual-slit unit cell," *Appl. Phys. Lett.* **96**(19), 191109 (2010).
10. M. Schubert, and F. Rana, "Analysis of Terahertz Surface Emitting Quantum-Cascade Lasers," *IEEE J. Quantum Electron.* **42**(3), 257–265 (2006).
11. J. A. Fan, M. A. Belkin, F. Capasso, S. Khanna, M. Lachab, A. G. Davies, and E. H. Linfield, "Surface emitting terahertz quantum cascade laser with a double-metal waveguide," *Opt. Express* **14**(24), 11672–11680 (2006).
12. S. Kumar, B. S. Williams, Q. Qin, A. W. Lee, Q. Hu, and J. L. Reno, "Surface-emitting distributed feedback terahertz quantum-cascade lasers in metal-metal waveguides," *Opt. Express* **15**(1), 113–128 (2007).
13. L. Mahler, A. Tredicucci, F. Beltram, C. Walther, H. E. Beere, and D. A. Ritchie, "Finite size effects in surface emitting Terahertz quantum cascade lasers," *Opt. Express* **17**(8), 6703–6709 (2009).
14. L. Mahler, A. Tredicucci, F. Beltram, C. Walther, J. Faist, H. E. Beere, D. A. Ritchie, and D. S. Wiersma, "Quasi-periodic distributed feedback laser," *Nat. Photonics* **4**(3), 165–169 (2010).
15. L. Mahler, A. Tredicucci, F. Beltram, C. Walther, J. Faist, B. Witzigmann, H. E. Beere, and D. A. Ritchie, "Vertically emitting microdisk lasers," *Nat. Photonics* **3**(1), 46–49 (2009).

1. Introduction

In external-cavity semiconductor lasers, tunable feedback is provided by the insertion of a controllable optical element such as a diffraction grating or a simple movable mirror. In the

former case, the frequency can be varied by changing the grating angle with respect to the incident beam, thereby shifting the frequency for maximum back-scattering; in the latter, the frequency of a Fabry-Perot resonator is tuned by a change of the external cavity length. In both situations a good design of the out-coupling optics is as essential as the suppression of unwanted reflections at the bare device facets, in order to maximize the contribution of the external cavity to the optical feedback.

The implementation of conventional external cavity concepts encounters difficulties in the case of terahertz semiconductor lasers [1,2], especially because the waveguide cross-sections are considerably smaller than the free-space wavelength. It is therefore challenging to efficiently couple the radiation to an external element and back into the waveguide. Nevertheless, with the development of appropriate techniques to suppress reflection on the laser facet, external cavity THz quantum cascade lasers were demonstrated using either a movable mirror to control the cavity length [3], or a rotating grating for wavelength dependent feedback [4]. In both cases, however, continuous tuning was limited to only a few GHz.

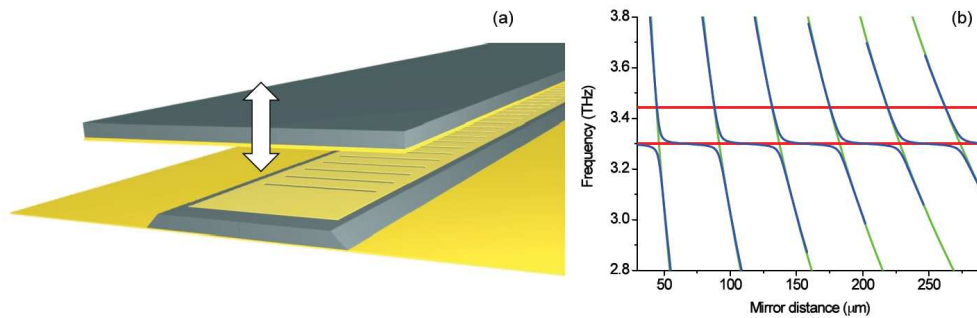


Fig. 1. (a) Schematic drawing of the experiment. The first resonator is formed by the grating along the double metal waveguide enclosing the gain material. The second resonator is formed by the patterned top metallization and the movable metallic mirror above. (b) Computed eigenfrequencies as a function of the mirror position above the grating. The separate eigenfrequencies of the DFB resonator and the metallic microcavity are plotted in red and green respectively. The DFB is formed by a dual-slit grating with the slits spaced by 70% of the period [9]. Considering the combined system (blue), the lower, vertically emitting band-edge of the DFB is strongly coupled to the metallic cavity where the two cavities share the same eigenfrequencies and therefore an anti-crossing is observed. The upper, non-radiative band-edge is not affected by the mirror and remains unchanged. In the calculation we assumed a 3.3 THz laser waveguide with a DFB grating period of 26 μm .

Here we present an external cavity laser that relies on an entirely different tuning mechanism. Instead of suppressing the feedback of the monolithic device and controlling the frequency that is fed back into the laser, we choose a geometry where an external cavity of size comparable to the wavelength is strongly coupled to the laser resonator. As the two systems are brought into resonance, the energy transfer established between them removes the degeneracy of their eigenfrequencies. Similar to the splitting of the eigenstates of two coupled oscillators, this eigenfrequency-splitting is determined only by the coupling strength, which is indeed quantified with the energy transfer rate between the resonators. By changing the size of the external microcavity, it should then be possible to tune the emission frequency of the laser over the eigenfrequency splitting, which is given by twice the energy transfer rate. The frequency tuning approaches realized up to now depend on effects like changes of material properties (typically the dielectric constant through temperature or gain pulling) [5,6], cavity length [3], or waveguide width [7], where the relative change of the given quantity leads to a proportional relative variation of the emission frequency. In contrast, the energy transfer rate is largely independent of the emission frequency, and thus the relative tuning range becomes larger for low frequency lasers [8].

Figure 1(a) shows a proof-of concept implementation of this idea. A vertically emitting terahertz quantum cascade laser is coupled to the microcavity formed by its top-metallization

and a closely spaced metallic mirror. Changing the position of the mirror tunes the eigenfrequencies of the microcavity in and out of resonance with respect to the fixed eigenfrequency of the laser resonator. The vertical emission is obtained from a distributed feedback (DFB) laser employing a metallic second-order grating [9–13]. The radiative surface losses of these devices depend on the symmetry of the DFB-eigenmodes with respect to the grating and the width of the slits in the top metallization. They can be increased by careful design of the boundary conditions at the waveguide end [10,12], or by the use of non-trivial grating concepts [9,14].

2. Modeling

In order to quantify the effect, we consider a strongly simplified system and use a commercial finite element solver (Comsol Multiphysics) to solve Maxwell's equations formulated as an eigenfrequency problem. Starting with a unit cell of an infinitely broad DFB-resonator with an air volume on top, we compute the eigenfrequencies while parametrically changing the distance d of the perfect electric conductor (mirror) acting as the boundary of the air above. As an example, the following calculations are carried out for a dual-slit DFB-device with a slit spacing/period ratio equal to 0.7, as described in [9]. The blue lines in Fig. 1(b) show the obtained eigenfrequencies, together with the band-edges of the undisturbed DFB unit cell and the microcavity eigenfrequencies given by the hyperbolae $n/(2d)$, where $n = 1,2,3\dots$. At the point where the microcavity is in resonance with the lower band-edge, the energy is transferred back and forth between the two resonators, and an anti-crossing of the two eigenfrequencies is observed. The energy transfer rate is determined by the surface losses of the DFB-resonator. The upper band-edge, whose symmetry of the eigenmode does not allow for vertical out-coupling, is not affected by the mirror.

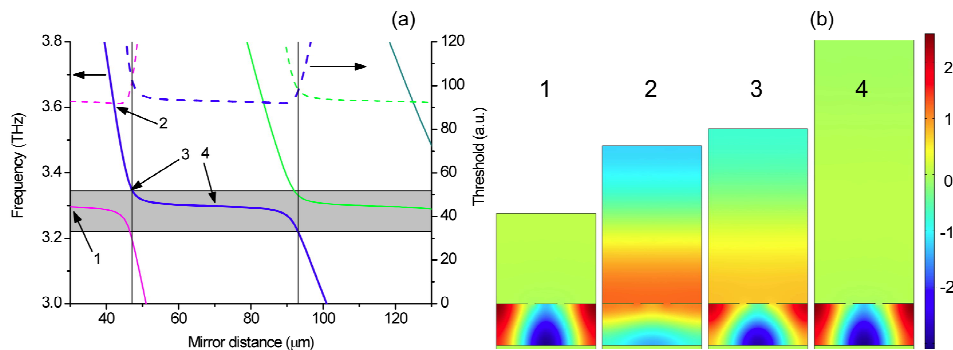


Fig. 2. (a) A few branches of of Fig. 1(b), plotted together with the respective threshold currents. According to this calculation, the blue branch would have the lowest threshold for mirror distances ranging from 47 to 93 μm (vertical lines), where the lasing frequency is tuned from 3340 GHz to 3220 GHz (grey rectangle) (b) Eigenmodes corresponding to the eigenfrequencies indicated with numbered arrows in panel (a). Mode 1 and 4 are not affected by the top mirror, and are thus DFB-like and entirely confined in the waveguide. Mode 2 is mostly microcavity-like, thus the confinement inside the active region is strongly reduced (~18%). At the anti-crossing point (3) the mode is equally distributed between waveguide and microcavity.

To estimate the potential tuning range, we also compute the ratio of ohmic losses and confinement, which determines the lasing threshold of a given eigenmode. This is plotted as a dashed line in Fig. 2(a) as a function of mirror-grating distance, together with the corresponding eigenfrequency. The electric field profile of the eigenmodes for four different mirror-positions is plotted in Fig. 2(b). Where the microcavity is not in resonance with the lower band edge of the DFB resonator, the DFB-like mode is unaffected and has a confinement factor close to unity. At the points of anti-crossing, the energy is distributed

between the two cavities, and the confinement factor is accordingly decreased, leading to a higher threshold. Assuming the laser always oscillates on the branch with the lowest threshold, we can estimate a potential tuning range of 120 GHz.

With a transparent top boundary, we obtained ~ 70 GHz surface losses [9] for such a structure, which confirms that the splitting or tuning range is determined by the surface losses and that it is about twice the energy transfer rate, as expected for coupled oscillators. We note, however, that it is presently unclear to which extent this simplified model of the DFB-resonator is able to accurately predict the surface losses of real devices [9]. In any case, the surface losses in these DFBs are mostly determined by the dual-slit spacing and by the ratio between emission wavelength and waveguide thickness (see Fig. 3). In principle much larger values can be achieved using thinner devices, though the practical implementation is more difficult, as the laser is unlikely to oscillate on the radiating DFB mode, at least in the absence of the external microcavity.

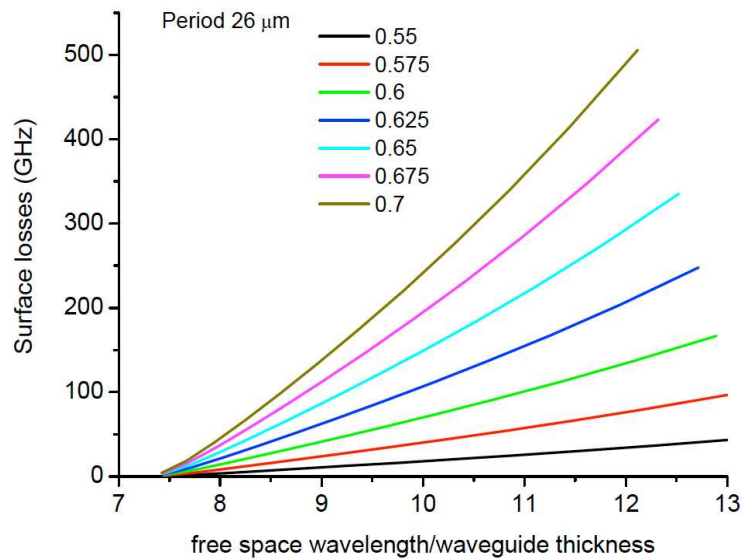


Fig. 3. Surface losses at 3.3 THz of a 26 μm dual-slit DFB grating as function of the ratio between wavelength and waveguide thickness. The different curves refer to the slit distance being a different fraction of the grating period.

3. Experiments

Experiments were carried out using a dual-slit DFB device operating in the fundamental lateral mode as already described in [9], with a slit-distance/period ratio of 0.7. It was mounted on a stepped copper bar, such that the wire bonds run as close as possible along the chip surface, in order to avoid contact with the mirror. The copper bar was in turn mounted upside down on the cold-finger of a continuous-flow liquid-helium cryostat for the measurements. Below the laser, the position of the horizontal metallic mirror (Cr/Au on GaAs) can be precisely controlled by an inertia piezo drive (Attocube ANPz51), which is also attached to the cold-finger [Fig. 4(a)]. It was driven with single 20 V saw tooth pulses. The laser was driven with an Avtech AVR-3HF-B power supply with pulses of 800 ns at 12.5 kHz and a 35 Ω resistor in series. The pumping current was set to 2.6 A, close to the point of maximum emission power. Spectra were recorded in the longitudinal direction with an $f/1$ Picarin lens and a Fourier transform infrared spectrometer in rapid scan mode, with a Si-bolometer detector, and at the maximum resolution of 0.125 cm^{-1} .

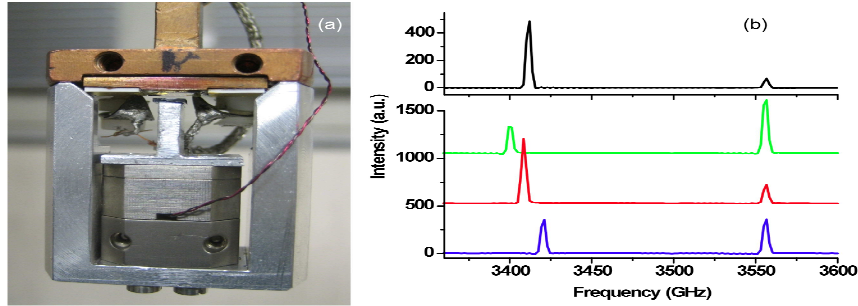


Fig. 4. (a) Experimental setup: The mirror is mounted face up on the inverted Aluminium-T, and is moved by the vertical piezo drive below towards the laser mounted upside down on the cold-finger of the cryostat (copper). The drive is in the fully retreated position here. (b) Top panel: Spectrum of a device without mirror. The two band-edges of the DFB-grating are observed. Bottom panel: Spectra with three different mirror positions. While the lower, vertically emitting band-edge clearly tunes with the mirror position, the upper band-edge is not affected by the top-mirror, exactly as predicted by the calculations shown in Fig. 2.

4. Results

The top panel of Fig. 4(b) displays the spectrum of a laser without any mirror mounted in the cryostat. The laser oscillates on both band-edges of the photonic band-gap, which is around 150 GHz wide, in good agreement with the modeling, especially considering that our linear eigenfrequency equations do not account for dispersion of the dielectric constant. The fact that both band-edges fall within the optical gain curve and are excited above lasing threshold is in contrast to devices with larger slit spacing, which were clearly single mode [9]. On the other hand this choice allows, by comparison of the behavior of the two emission peaks, an unambiguous demonstration of the proposed tuning mechanism. The three spectra in the bottom panel were derived from the same device but with the mirror placed at three different positions. Indeed the lower frequency peak clearly tunes symmetrically with respect to the position of the undisturbed peak. As expected, for the higher frequency one, no tuning is instead visible within the resolution of our spectrometer, a clear confirmation of its non-radiative character. From the simulations shown in Fig. 2, a continuous tuning of the lower band-edge should be observed; therefore, spectra were recorded for many closely spaced mirror positions. One pulse on the piezo-drive is estimated to move the mirror by a few hundred nm; typically 10 pulses were applied between two spectra. Figure 5 shows two such sequences. First, a series of spectra was recorded at an average mirror position of $\sim 500 \mu\text{m}$ [Fig. 5(a)]. The laser emission clearly tunes in a continuous manner over 10 GHz. This is considerably less than predicted by the modeling; our model, however, assumes that all the emitted energy is coupled back into the laser, which is clearly not the case for such a distant mirror. The deviation from the ideal case is difficult to estimate though, because the distance corresponds to the intermediate range between near- and far-field regime. Figure 5(b) then shows the spectra recorded for an average mirror distance of about one free-space wavelength. Here, the tuning range is already increased to 20 GHz. The figure also shows how the tuning occurs in branches, going from lower to higher frequencies, in very good agreement with the simulations of Fig. 2. In between the branches, no lasing is observed on the tuned band-edge. We attribute this to the increased threshold for the anti-crossing points displayed in Fig. 2(b). For this reason, we believe that, in this case, the relatively small tuning is rather due to the limited range of mirror positions for which the laser reaches threshold. In fact, comparing Fig. 5(b) to Fig. 2(b), we note that the region of mirror movement for which no lasing peak is observed is of about $10 \mu\text{m}$ between the branches, and this is exactly where the major tuning is predicted by the simulations. In this respect, the problem is probably made worse by the second lasing peak, on the non-radiative upper band edge [Fig. 4(b)], which lowers the

achievable gain for the desired radiative emission mode. A better gain material than the one presently used (a relatively standard 200-period phonon-depopulation design from the same wafer used in [15]) and a single-mode device would probably allow laser oscillation much closer to the anti-crossing point. Furthermore, we note that an improved management of the lateral beam divergence (for instance using a curved top mirror) could also improve the tuning range, especially for relatively large mirror-laser distances. However we think this is not the major limiting factor for low distances, as can be seen from the large threshold variation observed within each tuning branch, attesting that a large portion of the mode electromagnetic energy is indeed efficiently coupled between DFB and microcavity.

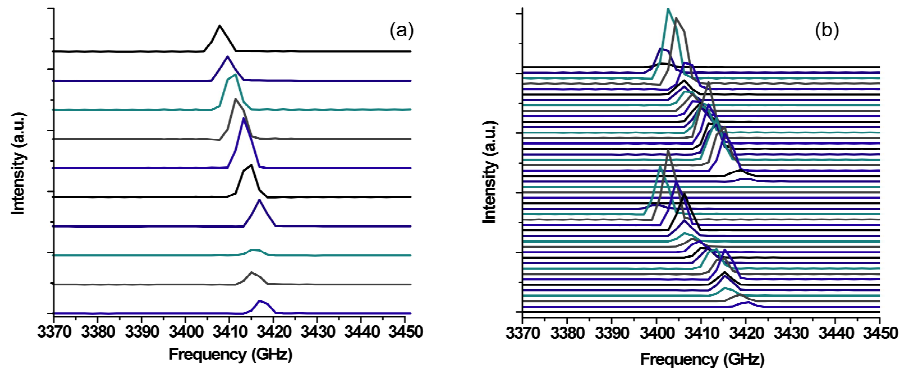


Fig. 5. Spectra collected from the laser driven with pulses of 800 ns at 12.5 kHz repetition rate and different mirror positions, with the mirror approaching the DFB from upper to lower spectra, where 200-250 steps of the piezo drive correspond to $\sim\lambda_0/2$ or 44 μm . (a) With the mirror at an average distance of $\sim 500 \mu\text{m}$, a tuning range of 10 GHz is observed while the mirror is moved by 120 steps. (b) With the mirror at a distance comparable to λ_0 , a tuning range of 20 GHz is observed. The mirror is moved by 10 steps between two consecutive spectra. Between the two branches, where no peak is observed, the laser oscillates only on the upper band-edge (not shown).

In Fig. 6 we report the L-I characteristics as measured from the device facet for different positions of the mirror. As already discussed above, near the anti-crossing point only the uncoupled upper band-edge DFB mode is lasing (black curve). Near the center of the tuning range instead (blue curve), the lower band edge mode is basically uncoupled from the external microcavity and almost entirely confined within the semiconductor, resulting in lasing with the lowest threshold. In intermediate positions (see the exemplary red curve), the confinement factor of the radiative mode goes down, because it starts spreading in the external microcavity, resulting in a threshold increase for this mode (corresponding to the kink in the red L-I). At the same time though, the slope efficiency improves significantly, probably because the waveguide losses decrease and the output is more collimated, as a consequence of the mode being less tightly confined and partly in vacuum. The behavior of the output power with mirror position at fixed current is reported in the inset of Fig. 6. The expected oscillations at half the wavelength period are indeed observed, with the main minima corresponding to the only upper DFB band-edge lasing and the secondary minima arising near the center of the tuning range where the slope efficiency of the lower band-edge mode is smaller. Overall we notice an increasing trend in power with decreasing distance of the movable mirror from the grating. This likely stems from the mirror becoming more and more effective in suppressing any residual radiation losses in the vertical direction (in fact the trend is more pronounced for the radiative mode).

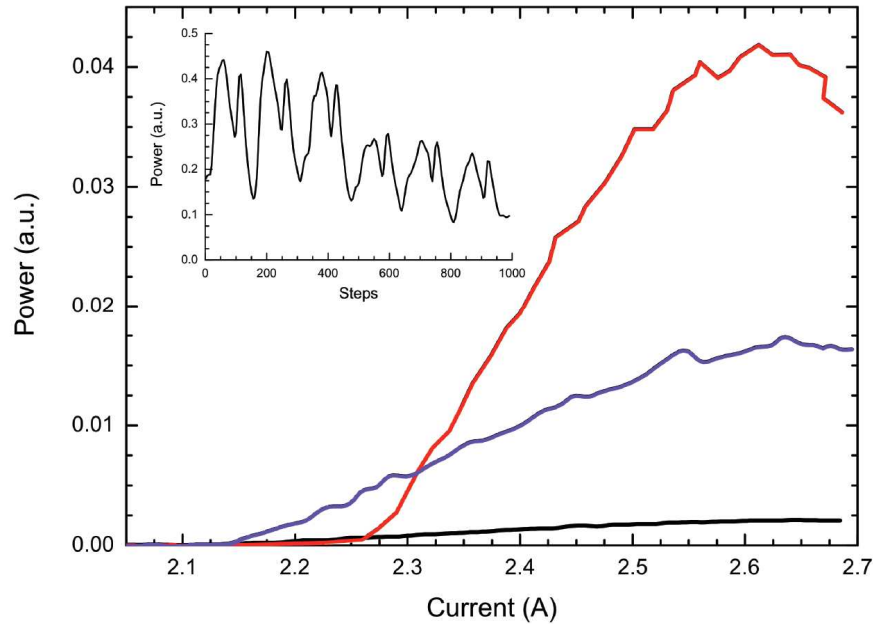


Fig. 6. Light-current (L-I) characteristics as measured from the device facet for the different positions of the top mirror: near the anti-crossing point between microcavity and radiative DFB mode (black), complete detuning (blue), intermediate (red). In the inset the output power at a current of ~ 2.6 A is plotted as a function of mirror movement, with zero being the closest position to the laser device. The magnitude of the piezo step depends on the exact temperature of the stage, friction, load etc. According to specifications, it should be of few hundred nm for the employed voltage.

At the moment the output powers achievable are comparable to those of conventional edge-emitting DFB lasers in double-metal waveguides, but, in the future, one could certainly exploit the capability of surface emission intrinsic of the concept to achieve large output powers, for instance through the use of a semi-transparent movable reflector.

5. Conclusions and perspectives

We have proposed a promising new idea for frequency tuning of semiconductor laser emission, especially suitable for low frequency lasers, and demonstrated its feasibility with a proof-of-concept experiment. For a larger tuning in THz QCLs, one could look for waveguide patterns with higher surface losses and work with more advanced gain material. More generally, one could search for other geometries of cavities with adjustable coupling, especially solutions where both resonators contain amplifying media, in order to avoid the low confinement factors that inhibit laser oscillation at the mode anti-crossing point, where the strongest tuning would be obtained. Furthermore, the intrinsically small volume of the additional cavity should make a future implementation of our concept realizable with MEMS-technology. Combining these efforts should lead to a very compact device that can be tuned over a large frequency range on short timescales.

Acknowledgments

We acknowledge Christoph Walther at ETH Zürich for help with the device processing. This work was supported in part by the European Commission through the Research and Training Network “Physics of Intersubband Semiconductor Emitters” and the integrated project “Teranova”. We also acknowledge support from the Italian Ministry of Research through the project “National Laboratory for Nanotechnology applied to Genomics and Post-Genomics”.